Pattern Recognition of White Matter Lesions Associated With Diabetes Mellitus Type 2

Jocellyn Luna * **Enrique Peláez** * **Francis R. Loayza** **
Ronald Alvarado *** **Maria A. Pastor** ****

* *Escuela Superior Politécnica del Litoral - ESPOL University, Faculty of Electrical and Computer Engineering, Guayaquil, Ecuador (e-mail: jmluna@espol.edu.ec, epelaez@espol.edu.ec)*
** *Escuela Superior Politécnica del Litoral - ESPOL University, Faculty of Mechanical and Production Sciences Engineering, Guayaquil, Ecuador (e-mail: floayza@espol.edu.ec)*
*** *Ministerio de Salud Pública - Guayaquil, Ecuador (e-mail: ronaldalvaradoczs5@gmail.com*
**** *Neuroimaging Laboratory CIMA, University of Navarra, Pamplona, Spain (e-mail: mapastor@unav.es)*

Abstract:
The White Matter Hyperintensities (WMHs) are usually associated with diabetes which is relevant in medical research to understand the long-term affection of diabetes. However, there is not enough evidence to distinguish whether the WMHs observed in diabetes subjects are structurally different from those observed in healthy subjects. This work aims to recognize the patterns associated with diabetes using the WMHs features of diabetic patients. We used Machine Learning models, such as Logistic Regression (LR), Support Vector Machines (SVM), Random Forest (RF), and a Multilayer perceptron (MLP) Neural Network to classify the features extracted from the WMH segments from T1 and FLAIR sequences of Magnetic Resonance Images (MRI) obtained from diabetic patients. Four classification models were evaluated and compared in their performance and Logistic Regression showed the best results, with an accuracy of 88%, as belonging or not to a diabetic class. Our results showed that diabetic patients have WMH patterns that are structurally different from controls, which may be useful for patients follow up.

Keywords: Diabetes, WMH brain lesions, machine learning, segmentation, classification.

1. INTRODUCTION

Diabetes mellitus type 2 is a chronic disease associated with problems in the carbohydrate metabolism. According to the World Health Organization, WHO (2016), in 2014 around 8.5% of adults in the world suffered from this disorder. Some causes that lead to diabetes are: depression, anxiety, and eating disorders, which are known as comorbidities of Diabetes, Ducat et al. (2014). Long-term effects of diabetes include retinopathy, diabetic neuropathy, diabetic ulcer, autonomic and sexual dysfunctions, as described by Singh et al. (2016). Furthermore, Biessels et al. (2006) indicates that patients with diabetes are more prone to developing dementia, due to some shared mechanisms with Alzheimer disease and changes in brain microvasculature.

The most common methods for diagnosing diabetes are clinical tests, such as sugar in urine and blood, glucose resistance, renal glucose threshold, intravenous and oral glucose resistance, Singh et al. (2016); however, due to the impact that diabetes has on brain morphology, studies point to using brain scanning for diabetes treatment and follow up, Moheet et al. (2015). One mechanism to identify structural changes and brain lesions caused by small vessel diseases is Magnetic Resonance Imaging (MRI), in different modalities, such as T1 weighted and FLAIR sequences, Christopher (2020); Saver *et al.* (2016). The White Matter Hyperintensities (WMH) are hyperintense brain regions, observed in fluid-attenuated inversion recovery (FLAIR) sequences of MRI, as part of the spectrum of small vessel diseases, such as hemorrhagic stroke, microbleeds and brain atrophy Maarten *et al.* (2012). These hyperintensities show brain lesions, caused by several diseases, including diabetes. Araki et al. (1994) found that WMH do not differentiate diabetic and non-diabetic patients. On the other hand, the presence of WMH in healthy subjects is commonly associated with aging, and it appears on subjects over sixty years old, as reported by Almkvist et al. (1992), but it has been also observed in a young healthy population, Hopkins et al. (2006). Additionally, it is well known that WMH is commonly related to diabetes, which is a major risk for cerebral infarction, Tamura and Araki (2015); however, it is poorly understood whether

the WMH observed in diabetes subjects are structurally different from those observed in healthy subjects. Therefore in this research, we propose the use of Artificial Intelligence (AI) algorithms to segment WMH, extract the features of the WMH's structural morphology, and then apply machine learning models to recognize and classify the patterns as belonging to a diabetic class or not.

This paper is organized as follows: Section 2 describes the methodology, as well as the data sets used in the experiments, their pre-processing, hyper-parameters settings, feature extraction, and a description of the environment used to implement the models; in Section 3, the proposed models' configurations are described; section 4 presents the results of the experiments using the proposed models; and, in section 5 some conclusions are drawn.

2. DATA AND METHODS

2.1 Imaging Data

For this work, three datasets containing MRI images were used: 1) A dataset of Ecuadorian subjects diagnosed with diabetes mellitus type II, extracted from the image database of a local MSP hospital in Ecuador, this dataset consisted of 64 pairs of MRI DICOM images per subject: T1 weighted (MPRAGE) and Fluid Attenued Inversion Recovery (FLAIR), which were anonymized using the conventional NIFTI format. The dataset contains images of patients diagnosed with diabetes mellitus type II. 2) A dataset containing 45 pairs of images from patients diagnosed with diabetes Mellitus type II, which were obtained from the Alzheimer Disease Neuroimaging Initiative (ADNI) database [1] ; and 3) A dataset with images from 41 healthy control subjects, obtained from the Neuroimaging Laboratory, University of Navarra from the studies described in Loayza et al. (2011); Aznárez-Sanado et al. (2013); Luis et al. (2015). A summary of the datasets can be seen in Table 1. In addition, demographic information was also recorded for each subject, as it is shown in Table 2, which describes the demographic data, such as: Age, sex, an internal ID and a unique identifier for the subject's MRI images.

Table 1. Number of subjects per type of image

Format	Diabetes	Healthy
FLAIR	109	41
T1	109	41

2.2 Preprocessing

Coregistration. Each pair of images per subject, were coregistered between them, using the SITK library, Insight Software Consortium (2020). Since each type could have different orientations and dimensions, in order to increase the number of slices, the FLAIR images were resliced to the T1 reference using a cubic interpolation procedure. The cubic interpolation reslicing technique used a third degree polynomial. We assume that points (x_i, y_i) and (x_{i-1}, y_{i-1}) can be represented by a cubic polynomial function, such as $f(x) = ax^3 + bx^2 + cx + d$ for every point $x_i <= x <= x_{i+1}$. To determine the coefficients a,b,c and d required by the cubic function, we used four points. When the values of the function $f(x)$ and its derivative at $x = 0$ and $x = 1$ are known, as it is expressed in (1).

$$f(y_0, y_1, y_2, y_3, x) = (-\tfrac{1}{2}y_0 + \tfrac{3}{2}y_1 - \tfrac{3}{2}y_2 + \tfrac{1}{2}y_3)x^3 + (y_0 - \tfrac{5}{2}y_1 + 2y_2 - \tfrac{1}{2}y_3)x^2 + (-\tfrac{1}{2}y_0 + \tfrac{1}{2}y_2)x + y_1 \quad (1)$$

Figure 1 shows the results of the interpolation, on the left there is a MPRAGE image, and on the right the FLAIR image, which has been overlapped with the MPRAGE image. As it can be seen the dimensions and orientation have been correctly adjusted.

[1] www.adni.loni.usc.edu

Table 2. Subject's demographic data

Group	Age (y)	Sex	Statistics
DMII	64.4	0.54	F=2.435, p=0.36
HCs	56.6	0.55	F=2.995, p=0.33

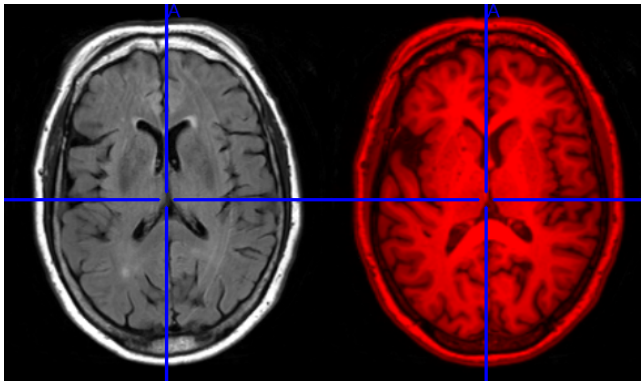

Fig. 1. MPRAGE and FLAIR image overlaid. Left image, the T1 weighted MPRAGE. Right in red, the overlaid FLAIR over the T1.

2.3 Segmentation

Once the images have been preprocessed, the next step consisted in segmenting the images, which allowed us to locate the WMH observed in FLAIR images; for this purpose a Convolution Neural Network (CNN) model with a U-net architecture was used. This architecture was originally created to recognize WHM patterns, as reported in Viteri J. and F. (2021), with an end-to-end architecture, which is able to recognize the lesions' patterns and to segment them from the FLAIR and T1 brain images. The result of applying this algorithm is a mask of WMH segments, as it is shown in red in Figure 2.

2.4 Feature Extraction

With the segments identifying the diabetes lesions in the brain images, the next step consisted in extracting the features that best described the segments; for performing this task we use the set of functions available in the Python SimpleITK library. The following filters and functions were applied to extract the features from the segmented binary mask images:

- Statistics Image Filter – used to extract statistical data, such as the average, mean, variance, maximum and minimum of each image segment.

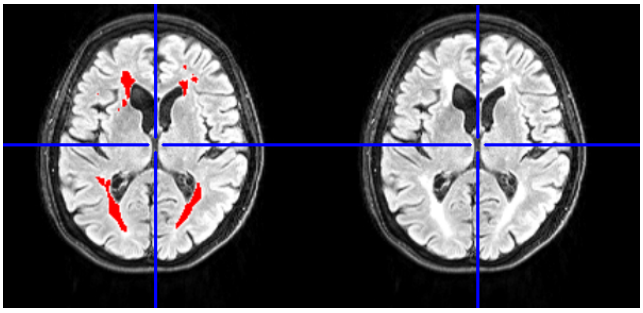

Fig. 2. WMH lesions segmentation. Left panel, in red the overlapped binary mask obtained by the U-net model. Right panel the FLAIR image

- Atan Image Filter – used to evaluate the inverse tangent function.
- Cos Image Filter – used to evaluate the cosine function.
- Morphological Watershed – filter used to perform morphological operations.
- Sobel Edge Detection Image Filter – used for 2D and 3D edge detection using the Sobel operator.
- Bounded Reciprocal Image Filter – used to filter with the function 1/(1+x).
- Zero-Crossing Based Edge Detection Image Filter – used for edge detection based on intensity variation.

To identify individual lesions in the binary masks, represented as 3D matrix, the following criteria was used:

(1) The mask is represented by a 3D matrix with variable dimensions, depending on the initial MRI.
(2) The absence of a lesion is represented by "0" and the presence by "1".
(3) The first lesion is identified in the first cell that has the value "1", and has not been previously categorized as part of another lesion.
(4) All adjacent and diagonal cells that have the value "1" are considered to be part of the lesion.
(5) If no more adjacent lesions are found, search for another cell with a value "1" not assigned to a lesion.

To identify the volume of the lesions, the number of cells that had a value "1" were added and multiplied by the value of the pixel volume. This volume can be assessed by multiplying the spaces, specified in the MRI metadata, giving an approximate volume of the lesions; then the total number of lesions and the average volume were calculated.

Considering a matrix M, which represents the MRI mask for a patient with dimension (x, y, z), the volume of a lesion is represented by (2):

$$\text{Pixel volume } V = (\sum_{i=1}^{x}\sum_{j=1}^{y}\sum_{k=1}^{z} M_{ijk}) \qquad (2)$$

2.5 Feature Selection

For selecting the features to be used in the classification process, a covariance matrix, such as the one represented in Figure 3, was used to rule out those characteristics that do not have a strong, or have a weak covariance with respect to the output variable, which in this case represents

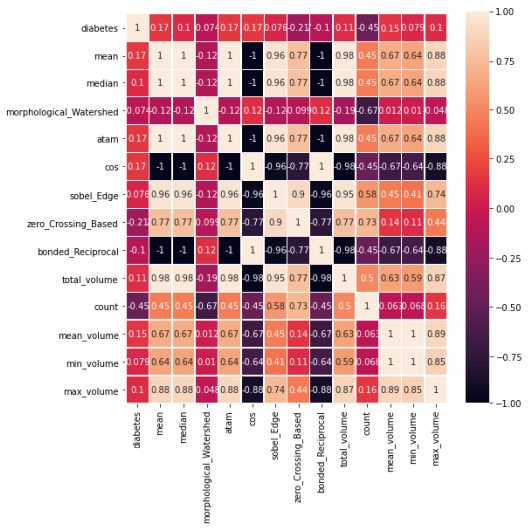

Fig. 3. Covariance matrix represented by a heatmap

the presence or absence of the patterns associated with diabetes.

From the analysis of the covariance matrix, the following selected features showed a strong relation with respect to the disease:

- The mean of the image.
- The mean after applying the inverse tangent function at each pixel.
- The mean after applying the Cosine Filter.
- The Zero-Crossing Based on Edge Detection.
- The mean volume of the segments.
- The number of lesions.

2.6 Implementation Environment

For extracting the features from the binary mask images, representing the segments, the following functions were used from the Python's SimpleITK library developed by Insight Software Consortium (2020):

- SITK: To read the images in DICOM and NIFTI formats.
- Numpy: To perform tensor and matrix operations.
- Scikit-Image: To perform dimension operations on images.
- Scikit-learn: To implement the classification models.

For implementing the deep learning models, used for segmenting the MRI images, we used Google-Collab (2020), as a virtual service with access to an Intel(R) Xeon(R) CPU @ 2.30GHz, with 1 core and 12 GB of RAM. The segmentation process for a set of MRI images, belonging to each patient, in this implementation environment took in average 43 seconds, which represents around 170 minutes for the 150 subjects.

3. CLASSIFICATION MODELS

After extracting the features from the segmented images, captured in the binary masks, the classification process was performed. For this process four classification models were evaluated and compared: a) Support Vector Machines

(SVMs); b) Random Forest (RF); c) Logistic Regression (LR); and, d) an MLP Neural Network.

Table 3. Relevant hyper-parameters setting for each model

Model	Hyper-parameters
Logistic Regression	solver = "lbfgs"
Support Vector Machine	kernel = "linear"
	gamma = ("scale", "auto")
Random Forest	n estimator = 1000
MLP	epochs = 30

The hyper-parameters used in these models are shown in Table 3. The solver parameter for the Logistic Regression model refers to the optimization algorithm used, in this case L-BFGS.

The gamma coefficient for the kernel used in the SVM model was set to 2.28e-05, after extracted from a grid search. For the RF model the n parameter estimator, representing the number of trees used, was set to 1000. For the MLP model, the number of training epochs was set to 30, after observing the behavior of *loss vs. the number of epochs*, where the validation accuracy began to decrease, and at the same time the loss started to increase.

3.1 Logistic Regression

Given the prediction problem we have is a binary classification task; that is, to predict the presence or absence of the patterns related to diabetes in a MRI image, we have chosen LR as one of the classification models, which can be designed to estimate a probability distribution of the expected prediction.

For implementing the LR model we used the Scikitlearn library version 0.22.2, available in Python. It computes the probability of finding the patterns, within the features extracted from the segments at the input MRI image, and assigns that probability value to the class labeled as *diabetes*. If the computed probability is grater than a threshold set to 0.7, the patient is diagnosed with diabetes, represented as 1, otherwise 0.

LR as a linear classifier, evaluates a linear function as it is expressed in (3):

$$f(x) = \beta_0 + \beta_1 X_1 + \beta_2 X_2 + \ldots \beta_k X_k \tag{3}$$

Where $x = (X_1, X_2 \ldots X_k)$ are the estimators of the regression coefficients and represent the features extracted from the segments used as inputs. The LR model is the Sigmoid function of *f(x)*, as defined by (4), which produces a value close to either 0 or 1. $\beta = (\beta_1, \beta_2 \ldots \beta_k)$ are the predicted weights or learned coefficients, such that the function *p(x)*, as defined in (4), is as close as possible to all predicted outputs, discovered from the input examples maximizing the Log-Likelihood (LL) function for all observations, which is represented by (5).

$$f(x) : p(x) = \frac{1}{1 + \mathrm{e}^{(-f(x))}} \tag{4}$$

$$LL = \sum_i (y_i log(p(x_i)) + (1 - y_i) log(1 - p(x_i))) \tag{5}$$

Where y_i denotes the predicted output and as before, x_i represents the features extracted from the segments of each MRI image.

3.2 Support Vector Machine

The Support Vector Machine (SVM) model used in this classification problem is based on a supervised learning strategy that maximizes a function with respect to an input collection of data, Noble (2006). The SVM model is focused in the separation of clusters with a hyperplane. However, it differs from other hyperplane-based classifiers by how the hyperplane is selected or discovered using a machine learning strategy; in this case the features extracted from the segments of each MRI image are used as the input, then it tries to maximize the margin of the vectors that define the hyperplane.

For implementing the SVM model, we have used the Sklearn SVC library available in Python, which discovers a hyperplane in a high-dimesional space; we use a linear kernel function to discover the hyperplane that best maximizes the expected margin. The Gamma value was set to 2.28e-05, given the linear kernel used for learning the hyperplane to fit the training dataset.

3.3 Random Forest

Caie et al. (2020) defines a Random Forest classifier as a two stage algorithm. In this work, the training phase involved the construction of several *"simple"* decision trees, then in the classification phase the decision is made by a majority of votes across those trees; hence, the output value is the average of the output values from the different decision trees assembled; in this case n, the number of decision trees estimator was set to 1000. As before a voting system was used to predict the presence or not of diabetes, which it has also been reduced to a binary classification problem.

3.4 MLP Neural Network

The Multi-Layer Perceptron (MLP) Neural Network, as defined by Du and Swamy (2014), is a full feedforward network that includes intermediate layers of units between the input and output layers. MLPs are commonly used for classification of linearly separable patterns as binary function approximators. For implementing the MLP we have used the Keras library version 2.4.3 available in Python. The MLP architecture was designed with 4 layers. The input layer was configured with 6 neurons corresponding to the number of input features; 2 hidden layers with 316 neurons; and, an output layer with one neuron, considering we face a binary classification problem. As activation function we used a Sigmoidal function, which allowed us to approximate the continuous function to a probability of the expected class.

4. RESULTS AND DISCUSSION

For training the models, and after preprocessing we selected the images of 110 subjects, with an average age of 56 years. From the 110 dataset, around 50% of the participants were women. Table 4 summarizes the characteristics of the subjects included in this research. In order to maintain a balance separation between training and testing groups, gender and the presence of diabetes features were used for fragmenting the dataset, obtaining a training group of 69 subjects and a testing group of 41 subjects.

Table 4. Participants Characteristics

Factor	
Number of subjects	110
Mean age	56.06
Number of female	51
Number of diabetic subjects	96
Number of healthy subjects	41

We used the co-variance matrix to determine and select the best candidate features, considering a correlation with the expected output label. Table 5 presents the selected categories with the highest variances among the features selected, which allowed us to discriminate the patterns observed in the segments extracted from the MRI images.

Table 5. Co-variance Matrix Results

	Diabetes
mean	0.17
atan mean	0.17
cos mean	0.17
zero-crossing	-0.21
mean volume	0.15
count of lesions	-0.45

After training and testing the models the accuracy score was calculated; Table 6 shows the results of the accuracy reached by each model, this score was used to compare the prediction performance of each model described in section 3, and as shown in the table, the LR model performed better than the other models, with an accuracy of 88.8%, sensitivity of 100% and specificity of 84%. Out of the 4 models, Random Forest has the lowest performance score with an accuracy of 79%. The selected characteristics or features used were: The image mean values, the mean value obtained after applying the inverse tangent function, the mean value obtained after applying the cosine function, the zero-crossing based edge mean value, the average lesion volume, and the number of lesions; these set of features showed a consistent result in predicting the presence of the disease patterns, that is if a subject is diabetic or not. The other classification models, SVM and the MLP Neural Network showed an average predictive performance, with an accuracy range between 0.818 and 0.848.

Table 6. Models Evaluation

Model	Accuracy
Logistic Regression	0.880
Support Vector Machine	0.848
Random Forest	0.790
MLP Neural Network	0.818

5. CONCLUSIONS

The Convolutional Neural Network with a U-Net architecture, created for segmenting WMH, showed a good performance after it was trained for recognizing and extracting the WMH patterns, associated with diabetes from the MRI Images, which later allowed us to discriminate the patterns that are structurally different from those observed in healthy subjects. The use of Machine Learning models allowed us to segment the WMH, extract the significant features of the WMH's structural morphology that characterized the diabetes lesions, and then recognize and classify those patterns.

Four machine learning models were evaluated and compared: Logistic Regression, Support Vector Machine, Random Forest and a 4 layer Multi Layer Perceptron; experimental results showed that Logistic Regression performed better than the other 3, with a prediction accuracy of 88% probability of belonging to the diabetic class or not. The sensitivity of 100% showed that the model do not have false negative predictions in the particular test dataset used, and specificity of 84% indicates the percentage of true negatives predictions.

The prediction consistency from all models showed that it could be possible to differentiate small vessel diseases, when comparing the WMH features, extracted from their segments, from both diabetic and non-diabetic patients.

From the recognized patterns associated to the small vessel lesions, it could be possible to train a model for recognizing the diabetes patterns from the MRI images, and discriminate between a subject diagnosed with diabetes from those with negative diagnosis, with an average accuracy of 83.4%.

Also, the results showed that the small vessel patterns learned, then recognized as brain lesions related to diabetes, could also indicate a long-term deterioration in medical areas that were not previously used to detect this disease.

ACKNOWLEDGEMENTS

We would like to thank the Alzheimer's Disease Neuroimaging Initiative (ADNI) (adni.loni.usc.edu), because part of the data used in this research was obtained from this database. The ADNI was launched in 2003 as a public-private partnership, led by Principal Investigator Michael W. Weiner, MD.

REFERENCES

Almkvist, O., Wahlund, L.O., Andersson-Lundman, G., Basun, H., and Bäckman, L. (1992). White-Matter Hyperintensity and Neuropsychological Functions in Dementia and Healthy Aging. *Archives of Neurology*, 49(6), 626–632. doi:10.1001/archneur.1992.00530300062011. URL `https://doi.org/10.1001/archneur.1992.00530300062011`.

Araki, Y., Nomura, M., Tanaka, H., Yamamoto, H., Yamamoto, T., Tsukaguchi, I., and Nakamura, H. (1994). Mri of the brain in diabetes mellitus. *Neuroradiology*, 36(2), 101–103.

Aznárez-Sanado, M., Fernández-Seara, M.A., Loayza, F.R., and Pastor, M.A. (2013). Functional asymmetries in early learning during right, left, and bimanual performance in right-handed subjects. *Journal of Magnetic Resonance Imaging*, 37(3), 619–631.

Biessels, G.J., Staekenborg, S., Brunner, E., Brayne, C., and Scheltens, P. (2006). Risk of dementia in diabetes mellitus: a systematic review. *The Lancet Neurology*, 5(1), 64–74.

Caie, P.D., Dimitriou, N., Arandjelovic, O., and Eng, M. (2020). Precision medicine in digital pathology via image analysis and machine. *Artificial Intelligence and Deep Learning in Pathology E-Book*, 149.

Christopher, M. (2020). Brain lesions: Causes, symptoms, treatments. Https://www.webmd.com/brain/brain-lesions-causes-symptoms-treatments. (Last accessed 7 November 2020).

Du, K.L. and Swamy, M. (2014). *Multilayer Perceptrons: Architecture and Error Backpropagation*. ResearchGate.

Ducat, L., Philipson, L.H., and Anderson, B.J. (2014). The mental health comorbidities of diabetes. *Jama*, 312(7), 691–692.

Google-Collab (2020). Google colaboratory. Last accessed: 20 October 2020. Available in: https://colab.research.google.com/notebooks/intro.ipynb.

Hopkins, R.O., Beck, C.J., Burnett, D.L., Weaver, L.K., Victoroff, J., and Bigler, E.D. (2006). Prevalence of white matter hyperintensities in a young healthy population. *Journal of Neuroimaging*, 16(3), 243–251.

Insight Software Consortium (2020). Simpleitk filters — simpleitk 1.2.0.dev documentation. `https://simpleitk.readthedocs.io/en/v1.2.4/Documentation/docs/source/filters.html`. Accessed: 2020-09-30.

Loayza, F., Fernández-Seara, M., Aznárez-Sanado, M., and Pastor, M. (2011). Right parietal dominance in spatial egocentric discrimination. *NeuroImage*, 55(2), 635–643. doi:https://doi.org/10.1016/j.neuroimage.2010.12.011. URL `https://www.sciencedirect.com/science/article/pii/S1053811910015934`.

Luis, E.O., Arrondo, G., Vidorreta, M., Martínez, M., Loayza, F., Fernández-Seara, M.A., and Pastor, M.A. (2015). Successful working memory processes and cerebellum in an elderly sample: a neuropsychological and fmri study. *PloS one*, 10(7), e0131536.

Maarten *et al.* (2012). Mri profile and response to endovascular reperfusion after stroke (defuse 2): a prospective cohort study - the lancet neurology. 316. Https://www.thelancet.com/journals/laneur/article/PIIS1474-4422(12)70203-X/fulltext. (Last accessed 31 October 2020).

Moheet, A., Mangia, S., and Seaquist, E.R. (2015). Impact of diabetes on cognitive function and brain structure. *Annals of the New York Academy of Sciences*, 1353, 60.

Noble, W.S. (2006). What is a support vector machine? *Nature biotechnology*, 24(12), 1565–1567.

Saver *et al.*, J. (2016). Time to treatment with endovascular thrombectomy and outcomes from ischemic stroke: A meta-analysis. *JAMA*, 316, 1279. Doi: 10.1001/jama.2016.13647.

Singh, N., Kesharwani, R., Tiwari, A., and Patel, D. (2016). A review on diabetes mellitus. *The Pharma Innovation*, 5, 36–40.

Tamura, Y. and Araki, A. (2015). Diabetes mellitus and white matter hyperintensity. *Geriatrics & gerontology international*, 15, 34–42.

Viteri J., Loayza F., P.E. and F., L. (2021). Automatic brain white matter hypertinsities segmentation using deep learning techniques. *Proceedings of the 14th International Joint Conference on Biomedical Engineering Systems and Technologies*, 4, 244–252.

WHO, W.H.O. (2016). Informe mundial sobre diabetes. *WHO*, 4.